31. THE STRONTIUM ISOTOPIC COMPOSITION OF PORE WATERS FROM LEG 133: NORTHEAST AUSTRALIAN MARGIN[1]

H. Elderfield,[2] P.K. Swart,[3] J.A. McKenzie,[4] and A. Williams[2]

ABSTRACT

Data are reported for strontium isotopic compositions of approximately 100 samples of pore waters recovered from the sediments of Ocean Drilling Program (ODP) Sites 812, 813, 814, 815, 817, 818, 823, and 824. Two types of pattern were found:

1. Sites 812 through 814 and 824 reflect a zoned system with the uppermost pore waters under diffusive control and with Sr concentrations and isotopic compositions controlled principally by dissolution of aragonite and the deeper pore waters affected by fluid flow with both Sr concentrations and $^{87}Sr/^{86}Sr$ ratios close to modern seawater values despite the Miocene age of the host sediment. It is possible that the fluid flow at depth is associated with a hardground between Pliocene/Pleistocene and Miocene/Pliocene sediments.

2. Pore waters from Sites 815, 817, 818, and 823 show increasing salinities/chloride with depth, which may reflect the presence of evaporites beneath the drilled sections. At Site 823, where porewater Sr concentrations reach nearly 3 mM, upward transport of Sr may be recognized from porewater $^{87}Sr/^{86}Sr$ ratios.

INTRODUCTION

Leg 133 of the Ocean Drilling Program provided a unique opportunity to study the evolution of the carbonate platforms of northeastern Australia (Fig. 1). Current knowledge about the evolution and diagenesis of carbonate platforms previously has come principally from work in the Caribbean (e.g., Mullins et al., 1984; Eberli and Ginsburg, 1989). One objective of the leg was to evaluate the diagenetic history and processes that operate on contrasting mixed carbonate/siliciclastic and pure carbonate margins in an environment considered to be undersaturated with respect to both aragonite and high-magnesium calcite at relatively shallow water depths.

A topic of particular importance was whether evidence for fluid flow through the carbonate platforms could be found. Mullins et al. (1984) and Simms (1984) proposed that the diagenesis of carbonate platforms can be controlled by fluid flow, resulting in the conversion of metastable minerals, such as high-magnesium calcite and aragonite, to low-magnesium calcite and the formation of dolomite. However, evidence for large-scale fluid flow was not found at previous ODP sites adjacent to carbonate platforms, such as in the Bahamas (Swart and Guzikowski, 1988) and the Maldives (Swart and Burns, 1990). Another topic of interest was that previous work on hemipelagic sediments drilled by ODP has shown evidence for the presence of evaporites at depth (Elderfield et al., 1991; Kastner et al., 1990) that can influence diagenetic processes.

Here, the results of measurements made of the $^{87}Sr/^{86}Sr$ ratios of Leg 133 pore waters are presented and a preliminary account is given of the processes defining the Sr isotope-depth profiles. Data for Sr isotopic compositions of pore waters provide important information about diagenetic processes (Elderfield and Gieskes, 1982). The Sr isotopic composition of seawater is known to have changed with time (Burke et al., 1982), with the result that Sr incorporated into primary carbonate minerals records the Sr isotopic composition of seawater of the age of deposition. In general, seawater $^{87}Sr/^{86}Sr$ ratios increased through the Cenozoic, although these rates of increase have varied significantly; thus, the seawater Sr isotope curve provides a template against which other data may be compared, either for an empirical assessment of age or to identify processes that have modified the expected changes in $^{87}Sr/^{86}Sr$ ratios with depth or time.

Changes in the Sr isotopic composition of seawater with time also are reflected in the depth profiles of pore waters, which tend to show decreasing $^{87}Sr/^{86}Sr$ ratios with depth, although the primary signal of buried seawater is modified by Sr diagenesis and transport. Recrystallization of primary carbonates results in the release of Sr to pore waters, modifying the shapes of the pore-water profiles (Baker et al., 1982; Richter and DePaolo, 1987). In general, in carbonate-rich sites, pore waters are characterized by Sr profiles that increase steeply with depth to concentrations up to an order of magnitude higher than seawater values (Elderfield and Gieskes, 1982), and $^{87}Sr/^{86}Sr$ ratios depart from values predicted from the age of the sediment by transport of Sr away from the zone of maximum recrystallization. Influx of Sr from nonseawater sources, such as volcanic ash or clay minerals, also changes $^{87}Sr/^{86}Sr$ ratios as does transport of Sr by advection from sources external to the sediments, such as from underlying oceanic crust (Baker et al., 1991), with the result that depth profiles of Sr isotope ratios provide a valuable method for identifying processes that modify sediments, especially when considered in conjunction with other pore-water and sediment chemistry and mineralogy.

METHODS

Pore waters were extracted using a stainless-steel Manhein-type squeezer (Sayles et al., 1973) at room temperature and filtered through 0.45 μm Gelman acrodisk disposable filters prior to shipboard analysis and storage of samples for shore-based analysis. The details of the shipboard procedures are summarized in the introduction and results of the shipboard analytical program are listed in the *Initial Reports*, Volume 133 (Davies, McKenzie, Palmer-Julson, et al., 1991).

Pore-water samples for Sr isotopic analysis were heat-sealed in plastic tubing after extraction and transported to Cambridge for analysis. Strontium was separated from 100 μL aliquots by conventional cation exchange chromatography and $^{87}Sr/^{86}Sr$ ratios determined using a VG Isomass 54E mass spectrometer equipped with a single collector (Elderfield et al., 1991). Some samples were analyzed using a VG Sector 54 instrument with seven collectors using a multidynamic peak
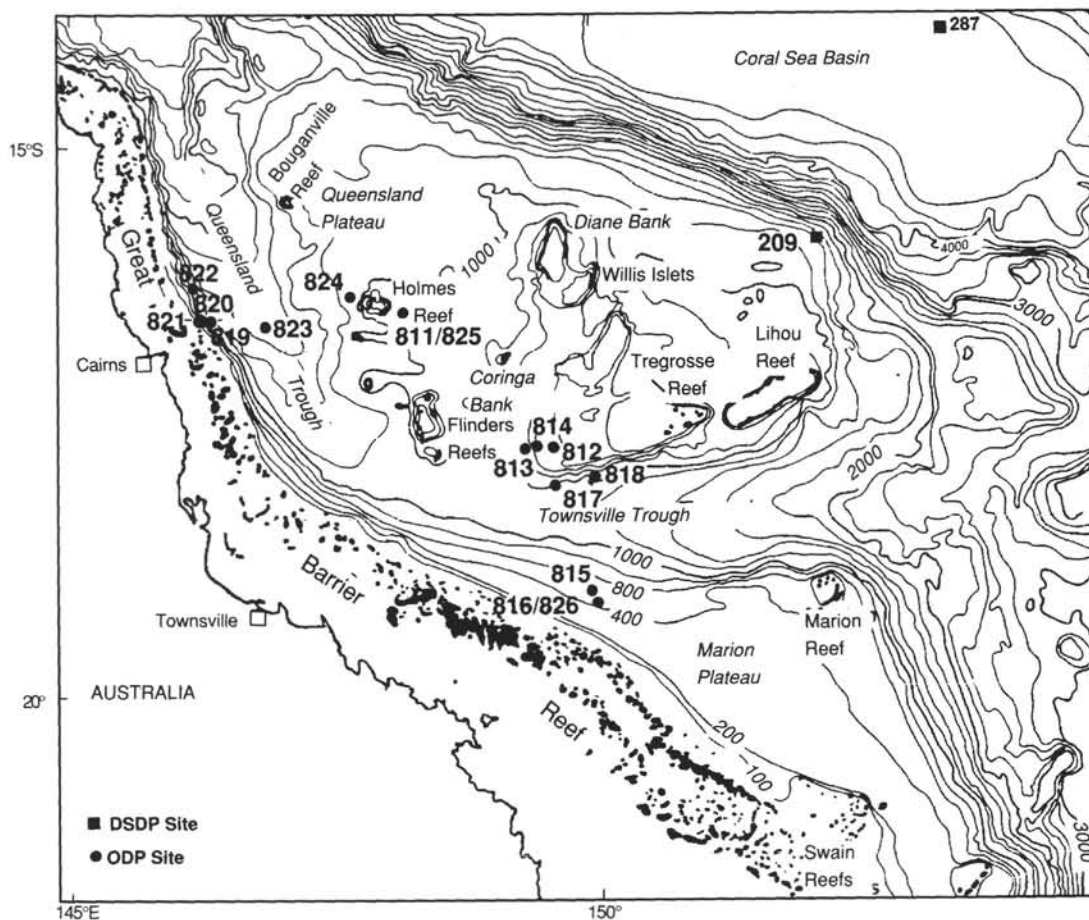
Figure 1. Map of study area showing positions of Leg 133 sites.

switching program. Results obtained for NBS 987 SrCO₃ standard during the course of the work gave $^{87}Sr/^{86}Sr = 0.71023$, and samples of an in-house seawater standard gave $^{87}Sr/^{86}Sr = 0.70917$.

RESULTS

Sr isotopic values were determined for a total of 97 pore-water samples from Sites 812, 813, 814, 815, 817, 818, 823, and 824, the locations of which are shown in Figure 1 and summarized in Table 1. Results are listed in Table 2, alongside shipboard data about Sr concentrations. Depth profiles of $^{87}Sr/^{86}Sr$ ratios and Sr concentrations in the pore waters are shown in Figures 2A through 2H.

Site 812

Site 812 is located on the southern margin of the Queensland Plateau between the Flinders and Tregrosse reefs. Together with Sites 813 and 814, it represents a transect across a platform-slope transition, with Site 812 being the lagoonal-bank end-member. The oldest sediment recovered was middle Miocene (189.9 mbsf) and the age of the oldest sediment from which pore water was obtained was late middle to early late Miocene (121.4 mbsf).

Strontium concentrations in pore waters (Fig. 2A) increase with increasing depth from above seawater values (~96 μM) to nearly 120 μM at 22 mbsf, below which concentrations decrease to constant values (103 μM), somewhat higher than the modern seawater concentration. The increase in pore-water Sr from the top of the hole to 22 mbsf is associated with a decrease in the aragonite content of the

sediment from ~50% at the top of the hole and its disappearance just below where pore-water Sr is at its maximum (Fig. 3A).

The decrease in pore-water Sr below ~25 mbsf is atypical of pore waters of carbonate-rich sediments drilled by DSDP/ODP, which normally show increases to constant Sr concentrations at depth (see Elderfield and Gieskes, 1982). The depth of the pore-water Sr maximum corresponds approximately to the Unit I/Unit II boundary (Davies, McKenzie, Palmer-Julson, et al., 1991). In Unit I of mainly Pleistocene age, $^{87}Sr/^{86}Sr$ ratios decrease with depth, similar to the changing $^{87}Sr/^{86}Sr$ ratio of seawater for this age range. However, below this boundary, $^{87}Sr/^{86}Sr$ ratios increase to values similar to those for modern seawater. $^{87}Sr/^{86}Sr$ ratios corresponding to the ages of the sediments (late Miocene to Pliocene) would be expected to decrease with depth to ~0.7089 (Fig. 4). As with the Sr data, this feature is unusual for carbonate-rich sediments.

Table 1. Leg 133 sites at which $^{87}Sr/^{86}Sr$ pore-water analyses took place.

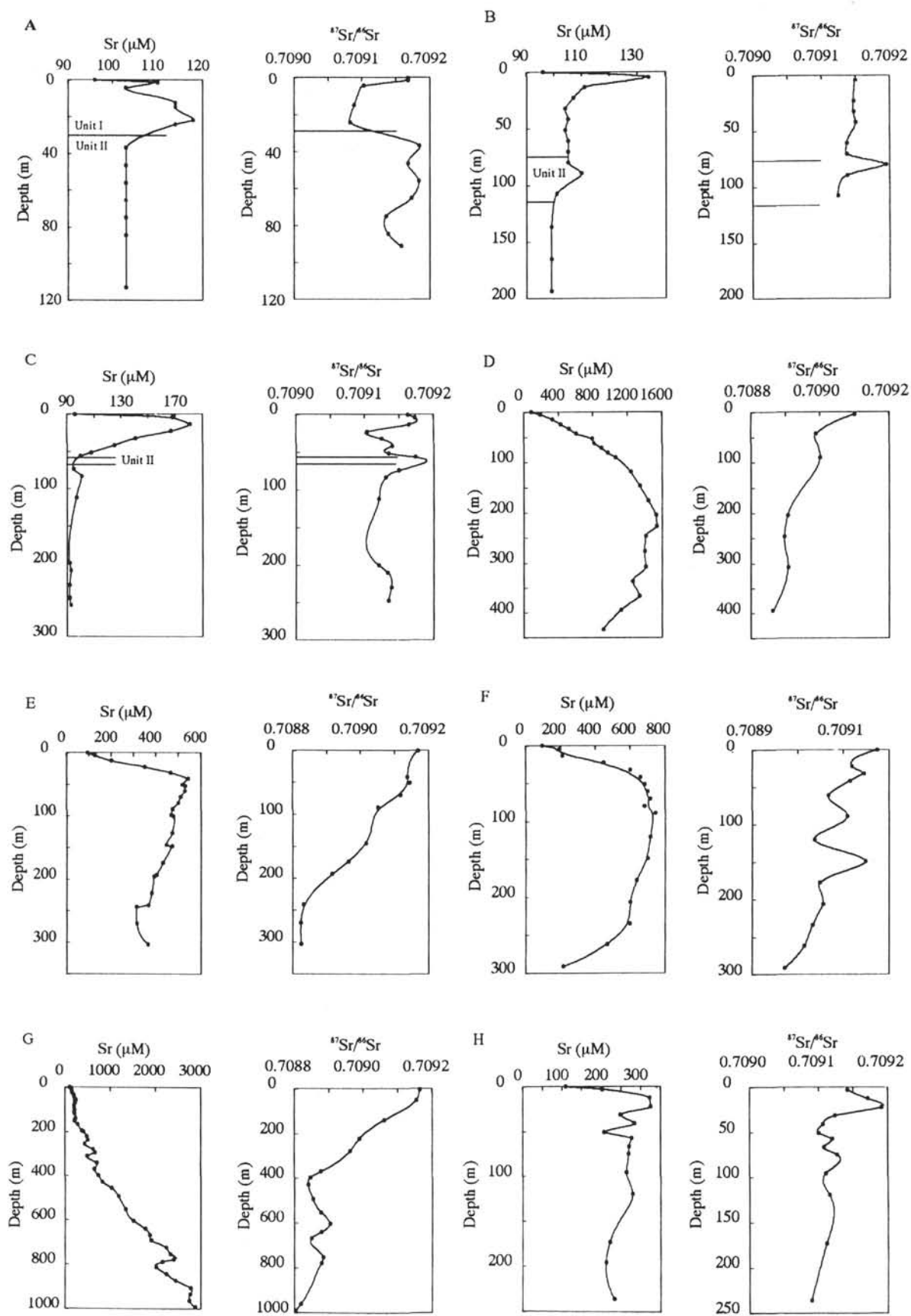| Site	Latitude	Longitude	Water depth (m)
812	17°48.84′S	149°36.31′E	937
813	17°49.95′S	149°29.67′E	539
814	17°49.99′S	149°30.83′E	520
815	19°09.03′S	149°59.51′E	466
817	18°09.49′S	149°45.50′E	1016
818	18°03.77′S	150°02.52′E	748
823	16°36.98′S	146°47.05′E	1638
824	16°26.70′S	147°45.73′E	1000

Figure 2. Depth profiles of Sr concentrations and $^{87}Sr/^{86}Sr$ ratios in Leg 133 pore waters. **A.** Site 812. **B.** Site 813. **C.** Site 814. **D.** Site 815. **E.** Site 817. **F.** Site 818. **G.** Site 823. **H.** Site 824.

Table 2. $^{87}Sr/^{86}Sr$ ratios and Sr concentrations of Leg 133 pore waters.

Core, section, interval (cm)	Depth (mbsf)	Sr (μM)	$^{87}Sr/^{86}Sr$ (±10⁶*2σ)
Site 812 Seawater	0	96	0.709168 (32)
133-			
812A-1H-1, 145–150	1.45	110	0.709168 (32)
812C-1H-3, 145–150	4.45	103	0.709103 (62)
812A-2H-5, 145–150	12.35	114	–
812C-2H-5, 145–150	14.8	114	0.709089 (78)
812A-3H-5, 145–150	21.85	118	–
812C-3H-5, 145–150	24.37	114	0.709083 (38)
812C-5H-5, 145–150	36.97	103	0.709185 (28)
812C-6H-5, 145–150	46.47	103	0.709168 (30)
812C-7H-5, 145–150	55.97	103	0.709184 (28)
812C-8H-5, 145–150	65.47	103	0.709173 (52)
812C-9H-5, 145–150	74.97	103	0.709136 (78)
812C-10H-5, 145–150	84.47	103	0.709139 (38)
812A-12X-5, 145–150	91.05	112	0.709158 (60)
812C-13H-5, 145–150	112.97	103	–
Site 813 Seawater	0	96	0.709160 (20)
133-813A-			
1H-3, 145–150	4.45	134	0.709149 (42)
2H-5, 145–150	13.17	111	–
3H-5, 145–150	22.67	107	0.709147 (24)
4H-5, 145–150	32.17	104	0.709147 (20)
5H-5, 145–150	41.67	105	0.70915 (24)
6H-5, 145–150	51.17	104	–
7H-5, 145–150	60.67	105	0.709137 (32)
8H-5, 145–150	70.17	105	0.709137 (18)
9H-5, 145–150	79.67	105	0.709194 (38)
10H-5, 145–150	89.17	110	0.709138 (20)
12H-5, 145–150	107.47	105	0.709124 (30)
15H-5, 145–150	136.67	99	–
18H-5, 145–150	165.17	99	–
21H-5, 145–150	193.67	99	–
Site 814 Seawater	0	96	0.709163 (20)
133-814A-			
1H-3, 145–150	4.45	168	0.709173 (26)
2H-5, 145–150	13.37	181	0.709165 (20)
3H-5, 145–150	22.87	167	0.709104 (26)
4H-5, 145–150	32.37	141	0.709125 (20)
5H-5, 145–150	41.87	125	0.70914 (24)
6H-5, 145–150	51.37	108	0.709135 (20)
7H-2, 145–150	56.3	100	0.709174 (6)
9H-5, 145–150	73.97	95	0.70915 (24)
10H-5, 145–150	83.47	101	0.709131 (18)
13H-5, 145–150	111.97	97	0.709121 (18)
23H-1, 145–150	200.1	92	0.709121 (20)
24H-2, 145–150	209.8	93	0.709134 (26)
26H-3, 145–150	230.2	92	0.709139 (20)
28H-2, 145–150	247.6	92	0.709135 (20)
29H-2, 145–150	257.2	93	–
Site 815 Seawater	0	86	0.709160 (20)
133-815A-			
1H-3, 145–150	4.45	193	0.709102 (22)
2H-5, 145–150	14.25	335	–
3H-5, 145–150	23.8	431	–
4H-5, 145–150	33.25	526	–
5H-5, 145–150	42.75	610	0.708989 (21)
6H-5, 145–150	52.25	798	–
7H-5, 145–150	61.75	817	–
8H-5, 145–150	71.25	897	–
9H-5, 145–150	80.75	973	–
10H-5, 145–150	90.2	1063	0.709001 (38)
13H-5, 145–150	118.7	1239	–
16H-5, 145–150	147.2	1347	–
19H-5, 145–150	175.7	1445	–
22H-3, 145–150	204.2	1534	0.708907 (21)
26X-3, 145–150	226.9	1541	–
28X-3, 145–150	246.2	1412	0.708897 (18)
31X-4, 145–150	276.7	1400	–
34X-5, 145–150	307.3	1414	0.708908 (21)
37X-5, 145–150	336.4	1261	–
40X-5, 145–150	365.5	1342	–
43X-5, 145–150	394.5	1124	0.708864 (21)
47X-5, 145–150	432.7	920	–
Site 817 Seawater	0	94	0.709170 (24)
133-817A-			
1H-3, 145–150	4.45	127	–
2H-5, 145–150	13.15	201	–
3H-5, 145–150	22.65	350	–
4H-5, 145–150	32.15	466	–
5H-5, 145–150	41.65	544	0.709138 (24)
6H-5, 145–150	51.15	517	0.709145 (26)

Core, section, interval (cm)	Depth (mbsf)	Sr (μM)	$^{87}Sr/^{86}Sr$ (±10⁶*2σ)
7H-1, 0–7	53.2	531	–
7H-5, 145–150	60.65	530	–
8H-5, 145–150	70.25	512	0.709118 (36)
9H-5, 145–150	79.65	500	–
10H-5, 145–150	89.15	475	0.709052 (24)
11H-5, 145–150	98.65	468	–
12H-1, 0–7	100.7	478	–
14H-5, 145–150	127.15	473	–
16H-5, 145–150	146.15	446	0.709016 (20)
17H-1, 0–7	148.2	472	–
19H-5, 142–150	174.62	432	0.708965 (20)
21H-5, 140–150	193.6	403	0.708916 (20)
22H-1, 0–7	195.7	393	–
24X-5, 140–150	222.1	382	–
26X-5, 140–150	241.4	367	0.708833 (18)
27X-1. 0–7	243.7	314	–
29X-5, 140–150	270.4	315	0.708824 (20)
5R-3, 140–150	303.4	365	0.708826 (30)
Site 818 Seawater	0	97	0.709173 (22)
133-818A-			
1H-4, 145–150	4.49	196	–
2H-5, 145–150	12.99	211	–
3H-5, 145–150	22.46	449	0.709118 (40)
4H-5, 145–150	31.99	603	0.709144 (20)
5H-5, 145–150	41.49	662	0.709114 (30)
6H-5, 145–150	50.99	685	–
7H-5, 140–150	60.49	704	0.709067 (26)
8H-5, 145–150	69.99	716	–
9H-5, 145–150	79.49	685	–
10H-5, 140–150	88.99	746	0.709108 (28)
13H-5, 140–150	120.53	716	0.709036 (24)
16H-5, 140–150	148.91	704	0.709148 (64)
19H-5, 140–150	177.5	638	0.709048 (20)
22H-5, 140–150	206	601	0.709055 (18)
25H-5, 140–150	234.51	599	0.709032 (36)
28H-5, 140–150	262	470	0.709014 (18)
31H-5, 140–150	291	217	0.708971 (21)
Site 823 Seawater	0	105	0.70916 (20)
133-823A-			
1H-3, 145–150	4.45	133	0.709165 (23)
2H-5, 145–150	13.25	148	–
3H-5, 145–150	22.75	157	–
4H-5, 145–150	32.25	190	–
5H-5, 145–150	41.75	202	–
6H-5, 145–150	51.25	218	0.709155 (18)
7H-1, 0–7	55.8	241	–
7H-5, 145–150	60.75	220	–
8H-5, 145–150	70.25	221	–
9H-5, 145–150	79.75	201	–
10H-5, 145–150	89.25	196	–
12H-1, 0–7	103.3	212	–
12H-5, 145–150	110.7	197	–
13H-5, 145–150	117.75	216	–
15X-5, 140–150	139.5	234	0.709062 (24)
17X-1, 0–7	151.4	211	–
18X-3, 0–7	165.5	282	–
21X-3, 140–150	194.6	374	–
22X-1, 0–7	199.8	409	–
24X-2, 140–150	221.6	477	0.70899 (26)
26X-1, 0–7	237.7	505	–
27X-6, 140–150	256.2	432	–
30X-2, 140–150	279.2	619	0.708962 (18)
32X-1, 0–7	295.6	662	–
33X-4, 140–150	311.2	494.5	–
36X-5, 140–150	341.6	703	–
39X-5, 140–150	370.4	654	0.708878 (26)
42X-4, 140–150	397.9	742	0.708846 (40)
45X-5, 140–150	428.3	825	0.70884 (30)
48X-4, 140–150	455.8	1029	–
52X-4, 140–150	493.7	1185	0.708855 (30)
58X-5, 140–150	552.8	1338	0.708878 (26)
64X-1, 135–150	604.55	1515	0.708904 (24)
67X-5, 135–150	639.55	1780	0.708879 (28)
70X-5, 110–125	667.75	1879	0.70885 (22)
73X-2, 135–150	692.45	1913	–
76X-4, 135–150	724.45	2248	–
79X-4, 135–150	753.45	2335	0.708884 (34)
82X-1, 135–150	778.05	2410	0.708879 (22)
1R-3, 130–150	788.3	2162	–
4R-1, 130–150	813.9	2023	–
7R-2, 130–150	844.5	2248	–
10R-1, 125–150	872.05	2444	–
13R-4, 130–150	905.6	2785	–

Table 2 (continued).

	Core, section, interval (cm)	Depth (mbsf)	Sr (μM)	^{87}Sr/^{86}Sr (±10^{6*}2σ)
	16R-4, 130–150	934.6	2774	–
	19R-3, 130–150	961.6	2750	0.708819 (18)
	22R-3, 130–150	990.5	2877	0.708804 (18)
Site 824 133-	Seawater	0	110	0.709160 (20)
	824B-1H-2, 145–150	2.95	203	0.709142 (26)
	824B-2H-5, 145–150	12.45	323	0.709172 (26)
	824B-3H-5, 145–150	21.95	326	0.709192 (26)
	824B-4H-5, 145–150	31.45	249	0.709124 (36)

Core, section, interval (cm)	Depth (mbsf)	Sr (μM)	^{87}Sr/^{86}Sr (±10^{6*}2σ)
824B-5H-5, 145–150	40.95	285	0.709107 (34)
824B-6H-5, 145–150	50.45	208	0.709100 (32)
824A-1H-5, 145–150	57.4	277	0.709120 (22)
824A-2H-5, 145–150	66.9	271	0.709108 (22)
824A-3H-4, 145–150	74.9	270	0.709127 (44)
824A-5H-5, 145–150	95.4	265	0.709111 (22)
824A-8H-2, 145–150	119.4	280	0.709116 (18)
824A-14H-5, 145–150	173.1	223	0.709112 (24)
824A-17X-2, 145–150	195.95	212	–
824A-21X-2, 145–150	235.6	234	0.70909 (28)

^{87}Sr/^{86}Sr ratios remain only slightly lower than that for modern seawater throughout the hole. There is a small shift from 0.70914 to 0.70915 within the top ~80 m and from 0.70912 to 0.70914 below ~90 m. The boundary zone corresponds approximately to where the small shift in pore-water Sr occurs, which is associated with the changes in lithology and physical properties at the boundaries of Unit II with Units I and III (Fig. 2B).

Site 814

Site 814 is located on the southwestern edge of the Tregrosse/Lihou/Coringa Bank complex, in front of a carbonate bank and represents the proximal transition between the lagoonal bank (Site 812) and the distal part (Site 813) of the three-site aggradational/progradational sequence. The oldest sediments recovered (300 mbsf) were middle Miocene or older.

The pore-water depth distributions of Sr and ^{87}Sr/^{86}Sr ratios (Fig. 2C) show similarities to those of the other transect sites, especially those of Site 812. Concentrations of Sr increase with depth and are associated with aragonite dissolution (Fig. 3A), and then decrease to a value slightly lower than that for seawater at ~50 mbsf, below which they remain constant over the interval sampled. The upper ~50 m (Unit I) is of Pleistocene to late Pliocene age, but pore-water ^{87}Sr/^{86}Sr ratios follow the seawater Sr isotope curve only for the top 23 m of the hole and then increase to a near-modern seawater value within Unit II, below which they decrease to near-constant values of ~0.70912 to 0.70914 over the remainder of the hole. As with Sites 812 and 813, these ratios are much higher than those for seawater of the age of the associated sediment (Fig. 4).

Site 815

Site 815 is located along the southern margin of the Townsville Trough, to the north and in front of the northwestern edge of the Marion Plateau. The hole consists of a thick, 473.5 m, sequence of Miocene-Pleistocene hemipelagic sediments overlying uppermost lower to upper Miocene shelf carbonates.

The pore-water Sr depth profile (Fig. 2D) is more typical of profiles normally seen from ODP sites than those described for Sites 812–814. However, profiles are complicated by the presence of elevated chloride concentrations and salinities, which, in general, show a near-linear increase with depth (Davies, McKenzie, Palmer-Julson, et al., 1991). Sulfate concentrations in the pore waters decrease over the upper ~200 m because of anoxic diagenesis but then, together with salinity, increase with depth for the remainder of the section. The Sr profile is the mirror image of that for sulfate and is probably controlled by it. The maximum concentration of Sr in pore waters is normally limited by celestite saturation, with the result that very high Sr concentrations can occur, as here, in association with sediments where dissolved Sr production is occurring in association with oxidation of organic matter by bacterial sulfate reduction.

^{87}Sr/^{86}Sr ratios in Site 815 pore waters decrease with depth from the modern seawater value to <0.7089 near the base of the hole. In contrast to the situation at Sites 812–814, these ratios are *lower* than
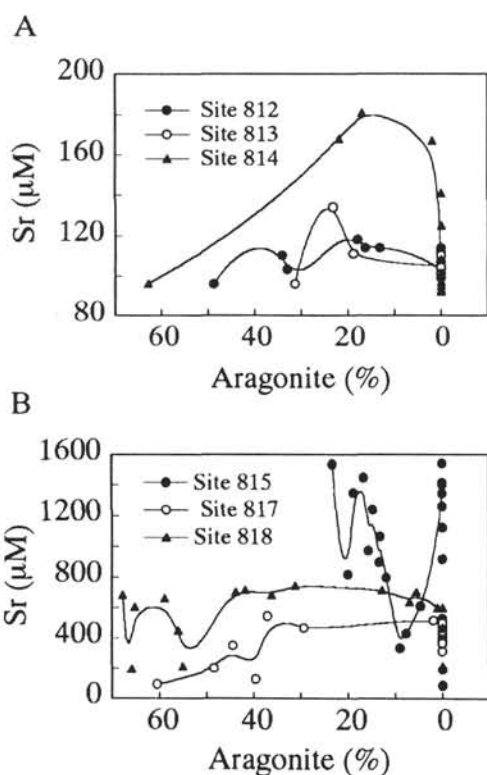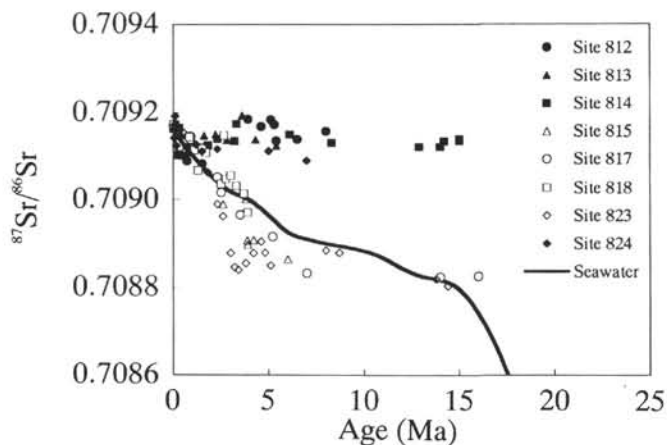

Figure 3. Plots of pore-water Sr concentrations vs. percentage of aragonite in sediments. **A.** Sites 812 through 814. **B.** Sites 815, 817, 818.

Site 813

Site 813 is located on the southwestern edge of the Tregrosse/Lihou/Coringa Bank complex and, with Sites 812 and 814, forms a three-site transect across a platform-slope transition, with Site 813 representing the most distal part of an aggradational/progradational sequence. As at Site 812, the oldest sediment recovered was middle Miocene in age.

Sr concentrations in the pore waters (Fig. 2B) exhibit features similar to those at Site 812. Concentrations increase to in excess of 130 μM at shallow depth (~5 mbsf) and then decrease to a constant value slightly above seawater concentration (~105 μM) down to ~107 mbsf. Below this, they decrease further to a constant value of ~100 μM. The zone of rapidly increasing pore-water Sr corresponds to that of aragonite dissolution and, as at Site 812, the increase in strontium is correlated with decreasing aragonite content of the sediment, such that the disappearance of aragonite occurs just below the pore-water Sr maximum (Fig. 3A).

The profile of ^{87}Sr/^{86}Sr ratio with depth is significantly different than that for the seawater Sr isotope curve (Fig. 4). As compared with the range between modern seawater and Miocene seawater values,

Figure 4. $^{87}Sr/^{86}Sr$ ratios of Leg 133 pore waters vs. age of sediments from which samples recovered, also showing the Sr isotope curve for seawater vs. time.

those corresponding to seawater of the age of the associated sediments (Fig. 4).

Site 817

Site 817 is situated on the northern side of the Townsville Trough, on the lower slope of the Queensland Plateau. Drilling recovered ~700 m of carbonate platform slope sediments from late early Miocene to Pleistocene age.

Sr concentrations in the pore waters (Fig. 2E) show some similarity to those at Site 815, although changes are less extreme. Concentrations increase to ~550 µM at ~60 mbsf and this upper zone is associated with decreases in aragonite from >60% at the top of the hole to zero at 53 mbsf (Fig. 3B). A very modest degree of sulfate reduction (~10% of seawater values) is found at this site, which limits the increase of pore-water Sr. Below ~60 mbsf, Sr concentrations decrease gradually with depth to 315 µM at 270 mbsf. As at Site 815, chloride and salinity increases occur in the deeper part of the hole (below ~120 mbsf). $^{87}Sr/^{86}Sr$ ratios in general parallel the changes in the seawater $^{87}Sr/^{86}Sr$ ratio for the age of the sediments (Fig. 4).

Site 818

Site 818 is located on an inclined terrace on the upper slope of the Queensland Plateau. Drilling recovered a 303 m-thick sequence of periplatform sediments of early Pliocene to Pleistocene age.

Depth profiles of Sr concentrations and $^{87}Sr/^{86}Sr$ ratios in pore waters (Fig. 2F) are similar to Sites 815 and, particularly, 817. Sr concentrations increase with increasing depth to ~70 mbsf and are associated with the disappearance of aragonite from the sediments (Fig. 3B). Below this depth, concentrations decrease in the zone of increased chloride concentrations and salinities. There is more significant sulfate reduction than was found at Site 817. Pore waters were saturated with respect to celestite between ~50 and 270 mbsf and celestite was found at ~180 and ~270 mbsf (Davies, McKenzie, Palmer-Julson, et al., 1991). $^{87}Sr/^{86}Sr$ ratios of the pore waters decrease with increasing depth to just <0.7090, higher than at Sites 815 and 817 in agreement with the age of the sediments (Fig. 4).

Site 823

Site 823 is located in the central western Queensland Trough, toward the deepest part of the basin. In excess of 1 km of core was recovered, comprising a sequence of middle Miocene to Pleistocene hemipelagic-pelagic sediments with numerous turbidites.

Concentrations of Sr in pore waters (Fig. 2G) are ~50% elevated, compared with seawater concentrations over the top ~140 m of the hole below which concentrations increase nearly linearly with depth to

almost 3,000 µM at the base of the core. This >30× enrichment over seawater values is exceptionally large and appears to result from a combination of intense bacterial sulfate reduction (pore-water sulfate reaches zero at ~50 mbsf and sulfate is near-absent [<2 mM] from most pore waters to a depth of ~700 m, below which it increases slightly to 5.6 mM at 990 mbsf) coupled with diagenesis of aragonite and high-Mg calcite, both of which are absent below ~300 mbsf (Fig. 3B).

$^{87}Sr/^{86}Sr$ ratios of pore waters decrease with depth from seawater to ~0.70885 at ~400 mbsf, below which they decrease more gradually and erratically with depth. The correspondence between $^{87}Sr/^{86}Sr$ ratios of pore waters and ratios equivalent to the sediment age (as derived from the seawater Sr isotope curve) is less straightforward than for Sites 815 and 816–818 (Fig. 4). Reasonably good correspondence is found at the base of the core, where pore-water $^{87}Sr/^{86}Sr$ ratios are similar to those of mid-Miocene seawater, but similar $^{87}Sr/^{86}Sr$ ratios of pore waters are also found at ~400 mbsf, in lower-upper Pliocene sediments (the $^{87}Sr/^{86}Sr$ ratio of Pliocene seawater is >0.7090).

Site 824

Site 824 is situated on the western slope of the Queensland Plateau, west of Holmes Reef. A total depth of 431 m was drilled until upper Oligocene-lower Miocene sediments, where basement, probably of Paleozoic age, was reached.

Sr concentrations in pore waters (Fig. 2H) increase to ~325 µM at ~22 mbsf, but then decrease to ~250 µM at depth, with slightly higher values, on average, between 22 and 150 mbsf than deeper in the hole. The increased Sr is associated with dissolution of aragonite; however, unlike other sites, aragonite persists to much deeper in the sediment (Fig. 3A).

$^{87}Sr/^{86}Sr$ ratios of pore waters from the top 22 m of the hole are analytically indistinguishable from modern seawater, and then decrease abruptly to a constant value of ~0.70911 for the remainder of the section sampled. This value is equivalent to that for Pliocene-Pleistocene seawater, although the sediments are much older.

DISCUSSION

It is possible to categorize the sites into two groups on the basis of the pore-water results described in the previous section: (1) Sites 812 through 814 and 824; and (2) Sites 815, 817 through 818, and 823. The Group 1 sites are of particular interest in that the pore-water data reflect the presence of fluid flow. The Group 2 sites share the characteristic that they exhibit the possible influence of buried evaporites.

Evidence for Fluid Flow

In summary, the coupled Sr concentration/isotopic composition results for pore waters from Sites 812 through 814 and 824 (Figs. 2A–2C, 2H) may be described as a zoned system. In the upper layer, Sr concentrations increase and $^{87}Sr/^{86}Sr$ ratios decrease with depth as a consequence of aragonite dissolution. However, the elevated Sr concentrations do not persist with increasing depth and $^{87}Sr/^{86}Sr$ ratios do not decrease further, as would be expected. Despite the observation that aragonite dissolution is complete at shallow sub-bottom depths, pore-water Sr concentrations return to near-seawater values at depth (the lower layer). The rapid disappearance of aragonite (within the Pleistocene sections) is indicative of rapid recrystallization of aragonite to calcite, yet pore-water Sr concentrations are similar to seawater values in the lower layer. This observation implies that the upper layer is diffusion-reaction-dominated (aragonite dissolution and diffusive Sr transport), whereas the lower layer is advection-dominated because of fluid flow.

The Sr isotope data strongly support this interpretation. In the upper layer, $^{87}Sr/^{86}Sr$ ratios follow changes in seawater Sr isotopic composition, but in the lower layer the pore waters of near-seawater Sr concentrations have $^{87}Sr/^{86}Sr$ ratios that are similar to modern

seawater values. This observation supports the suggestion that fluid flow through carbonate platforms provide a mechanism for the supply of chemical constituents to drive diagenetic reactions (Mullins et al., 1984; Simms, 1984).

Temperature measurements at Sites 812 and 814 provide additional support for fluid flow (Davies, McKenzie, Palmer-Julson, et al., 1991). At Site 812, temperatures are near constant at 10°C to a depth of 225 mbsf and then rise abruptly to 17.6°C at 300 mbsf, suggesting that water may be drawn through the sediments. At Site 814, there is a sharp temperature gradient near the sediment/seawater interface that is suggestive of water flow out of the sediments. However, there are significant uncertainties associated with the interpretation of downhole temperature measurements and there are inconsistencies between the idea of vertical flow and the pore-water data which imply a lateral component to flow. For example, the $^{87}Sr/^{86}Sr$ ratio minimum at 20 mbsf in Site 812 (Fig. 2A) is strongly suggestive of lateral flow. Similarly, if Ca in pore waters at Site 814 (Davies, McKenzie, Palmer-Julson, et al., 1991) is more-or-less conservative, then the flow must be very slow.

The presence of hardgrounds or lithological boundaries may provide the flow paths for such fluid flow. Considering the transect represented by Sites 812–814–813 (Figs. 2A, 2C, and 2B), one can see that at Site 812 the zone boundary corresponds to a hardground between sediment Units I and II. At Site 814, a hardground (Unit II) corresponds to the depth of the zone boundary at ~70 mbsf where the maximum in $^{87}Sr/^{86}Sr$ occurs. At Site 813, there is no hardground and the upper ~75 m of the sediment is characterized by pore waters with the same $^{87}Sr/^{86}Sr$ ratio, despite the strong gradient in Sr concentration. At this site, the upper and lower boundaries of Unit II are characterized by changing physical properties (Davies, McKenzie, Palmer-Julson, et al., 1991) and the Sr and $^{87}Sr/^{86}Sr$ profiles are sensitive to such changes. Tracing the outcrop of the hardgrounds on the platform using seismics is a possible next step to evaluating the pathways of fluid flow.

One method of estimating the rate of fluid flow is to calculate the water movements necessary to eradicate Sr concentration anomalies from aragonite dissolution of the magnitudes seen in the upper zones at these sites. Such values will be minimum rates. The Sr concentration gradients shown in Figure 2 for these sites range from ~1 to 8.5 μM/m. Assuming a diffusion coefficient for Sr of ~100 cm²/yr gives fluxes of ~1 to 8 μmol/cm²/k.y. The minimum water fluxes required to eradicate pore-water Sr anomalies driving these fluxes are 0.05 to 0.2 cm/yr. An alternative method is through use of the Peclet number, P_e (see Bickle and McKenzie, 1987), as

$$P_e = W_o / h \cdot D_f, \qquad (1)$$

where h = the thickness of the zone of diffusive mixing, W_o = the volume fluid flow per unit area, and D_f = the effective diffusivity. Systems having values of $P_e < 1$ are diffusion-dominated, and those having $P_e > 1$ are advection-dominated. Taking Site 813 as an example, where $^{87}Sr/^{86}Sr$ data imply that mixing between the region of fluid flow and overlying seawater occurs over a subsurface depth range of ~4 m, and assuming $P_e = 10$, gives a flow rate of 2.5 cm/yr. Both methods of estimation are crude but provide order-of-magnitude values of *minimum* flow rates through the carbonate platform.

The Influence of Evaporites

Increases in chloride concentrations of pore waters with depth appear to be a common feature in the Miocene/Pliocene sediments of the Queensland and Townsville troughs and have been observed at Sites 815, 817, 818, 822, and 823. Evaporites are not known for these basins but evaporites have been identified in Oligocene sediments of the Capricorn Basin at ~25°S (Ericson, 1976). Thus, it is possible that the chloride gradients reflect transport from evaporites associated with Oligocene strata at the ODP sites, which have been identified from seismic sections (Davies, McKenzie, Palmer-Julson, et al.,

1991). It has been suggested that during the post-breakup subsidence of the troughs, partially restricted shallow-marine conditions existed.

It is difficult to recognize evidence for the influence of the evaporites from pore-water Sr and $^{87}Sr/^{86}Sr$ data. For the majority of sites, $^{87}Sr/^{86}Sr$ ratios of pore waters appear to be controlled by diagenetic reactions within the sediment column. At Site 823, the pore-water profiles are indicative of a supply of Sr from below. The uppermost ~150 m of the pore-water system appears to be in diffusive communication with the overlying water column but, at depth, $^{87}Sr/^{86}Sr$ ratios suggest upward transport of Sr from underlying sediments. If this feature reflects influx from evaporites, then the results may be considered in terms of two-end-member mixing, assuming that Sr behaves conservatively. However, this limits the end-member $^{87}Sr/^{86}Sr$ ratio only to ~0.70875 (~15 Ma). Work during ODP Leg 112 (Peru margin), where high chlorinities at depth were also observed (Kastner et al., 1990; Elderfield et al., 1991), showed that profiles were consistent with the mixing of an evolved brine associated with evaporite formation with the seawater as it was transported at depth within the marginal sediments. Thus, the high-chloride end-member at a particular site may be itself a mixture of brine and seawater that is in diffusive communication with the overlying pore-water system. Therefore, the end-member Sr isotopic composition of the high-chloride end-member when translated to an isotopic age will always be younger than the age of the evaporite.

SUMMARY

The most important result obtained during this preliminary study of the Sr isotopic compositions of pore waters from Leg 133 has been the evidence that they provide for fluid flow through the Queensland Plateau. The combination of Sr concentrations at depth similar to seawater values and $^{87}Sr/^{86}Sr$ ratios similar to values for modern seawater associated with sediments of Miocene age provides an important first piece of definitive evidence of fluid flow through a carbonate platform, a process that often has been suggested to be important for carbonate diagenesis. The pore-water profiles showing such features (Sites 812 through 814, and 824) are atypical of pore-water profiles previously seen at DSDP/ODP sites and are important in that they represent the first detailed profiles of Sr isotopes in a transect of a carbonate platform. Profiles at other Leg 133 sites are more typical of Sr isotope profiles described from earlier work.

ACKNOWLEDGMENTS

REFERENCES[*]

Baker, P.A., Stout, P.M., Kastner, M., and H. Elderfield, 1991. Large-scale advection of seawater through oceanic crust in the central equatorial Pacific. *Earth Planet. Sci. Lett.,* 105:522–533.

Bickle, M.J., and McKenzie, D., 1987. The transport of heat and matter by fluids during metamorphism. *Contrib. Mineral. Petrol.,* 95:384–392.

Burke, W.H., Denison, R.E., Hetherington, E.A., Koepnick, R.B., Nelsen, H.F., and Otto, J.B., 1982. Variation of seawater $^{87}Sr/^{86}Sr$ ratio throughout Phanerozoic time. *Geology,* 10:516–519.

[*] Abbreviations for names of organizations and publication titles in ODP reference lists follow the style given in *Chemical Abstracts Service Source Index* (published by American Chemical Society).

Davies P.J., McKenzie, J.A., Palmer-Julson, A., et al., 1991. Introduction. *In* Davies, P.J., McKenzie, J.A., Palmer-Julson, A., et al., 1991. *Proc. ODP, Init. Repts.,* 133: College Station, TX (Ocean Drilling Program), 5–30.

Eberli, G.P., and Ginsburg, R.N., 1989. Cenozoic progradation of the northwestern Great Bahamas Bank. *Soc. Econ. Paleontol. Mineral. Spec. Publ.,* 4:339-351.

Elderfield, H., and Gieskes, J.M., 1982. Sr isotopes in interstitial waters of Deep Sea Drilling Project cores. *Nature,* 300:493–497.

Elderfield, H., Kastner, M., and Martin, J.B., 1991. Compositions and sources of fluids in sediments of the Peru subduction zone. *J. Geophys. Res.,* 95:8819–8827.

Ericson, E.K., 1976. Capricorn Basin. *Econ. Geol. Austral. Papua New Guinea,* Vol. 3, 7:446–450.

Kastner, M., Elderfield, H., Martin, J.B., Suess, E., Kvenvolden, K.A., and Garrison, R.E., 1990. Diagenesis and interstitial-water chemistry at the Peruvian continental margin—major constituents and strontium isotopes. *In* Suess, E., von Huene, R., et al., *Proc. ODP, Sci. Results,* 112:413–440.

Mullins, H.T., Heath, K.C., Van Buren, M., and Newton, K., 1984. Anatomy of a modern open-oceanic carbonate slope: northern Little Bahama Bank. *Sedimentology,* 31:141–168.

Richter, F.M., and DePaolo, D.J., 1987. Numerical models for diagenesis and the Neogene Sr isotopic evolution of seawater from DSDP Site 590B. *Earth Planet. Sci. Lett.,* 83:27–38.

Sayles, F.L., Manheim, F.T., and Waterman, L.S., 1973. Interstitial water studies in small core samples. *In* Heezen, B.C., MacGregor, I.D., et al., *Init. Repts. DSDP,* 20:783–804.

Simms, M., 1984. Dolomitization by groundwater sytems in carbonate platforms. *Trans. Gulf Coast Assoc. Geol. Soc.,* 34:411–420.

Swart, P.K., and Burns, S.J., 1990. Pore-water chemistry and diagenesis in sediments from Leg 115: Indian Ocean. *In* Duncan, R.A., Backman, J., Peterson, L.C., et al., *Proc. ODP, Sci. Results,* 115:629–645.

Swart, P.K., and Guzikowski, M., 1988. Interstitial-water chemistry and diagenesis of periplatform sediments from the Bahamas, ODP Leg 101. *In* Austin, J.A., Schlager, W., et al., *Proc. ODP, Sci. Results,* 101:363–380.